

# Novel mesoporous silica-based antibiotic releasing scaffold for bone repair

Xuetao Shi<sup>a,b,1</sup>, Yingjun Wang<sup>a,c,\*,1</sup>, Li Ren<sup>a,c</sup>, Naru Zhao<sup>a,c</sup>,  
Yihong Gong<sup>b</sup>, Dong-An Wang<sup>b,c,\*</sup>

<sup>a</sup> School of Materials Science and Engineering, South China University of Technology, Guangzhou 510641, China

<sup>b</sup> Division of Bioengineering, School of Chemical and Biomedical Engineering, Nanyang Technological University, Singapore 637457, Republic of Singapore

<sup>c</sup> Key Laboratory of Specially Functional Materials and Advanced Manufacturing Technology, South China University of Technology, Ministry of Education, Guangzhou 510641, China

Received 25 August 2008; received in revised form 25 December 2008; accepted 5 January 2009

Available online 23 January 2009

## Abstract

Tissue engineering scaffolds with a micro- or nanoporous structure and able to deliver special drugs have already been confirmed to be effective in bone repair. In this paper, we first evaluated the biomineralization properties and drug release properties of a novel mesoporous silica–hydroxyapatite composite material (HMS–HA) which was used as drug vehicle and filler for polymer matrices. Biomineralization can offer a credible prediction of bioactivity for the synthetic bone regeneration materials. We found HMS–HA exhibited good apatite deposition properties after being soaked in simulated body fluid (SBF) for 7 days. Drug delivery from HMS–HA particle was in line with Fick's law, and the release process lasted 12 h after an initial burst release with 60% drug release. A novel tissue engineering scaffold with the function of controlled drug delivery was developed, which was based on HMS–HA particles, poly(lactide-co-glycolide) (PLGA) and microspheres sintering techniques. Mechanical testing on compression, degradation behavior, pH-compensation effect and drug delivery behavior of PLGA/HMS–HA microspheres sintered scaffolds were analyzed. Cell toxicity and cell proliferation on the scaffolds was also evaluated. The results indicated that the PLGA/HMS–HA scaffolds could effectively compensate the increased pH values caused by the acidic degradation product of PLGA. The compressive strength and modulus of PLGA/HMS–HA scaffolds were remarkably high compared to pure PLGA scaffold. Drug delivery testing of the PLGA/HMS–HA scaffolds indicated that PLGA slowed gentamicin sulfate (GS) release from HMS–HA particles, and the release lasted for nearly one month. Adding HMS–HA to PLGA scaffolds improved cytocompatibility. The scaffolds demonstrated low cytotoxicity, and supported mesenchymal stem cells growth more effectively than pure PLGA scaffolds. To summarize, the data supports the development of PLGA/HMS–HA scaffolds as potential degradable and drug delivery materials for bone replacement.

© 2009 Acta Materialia Inc. Published by Elsevier Ltd. All rights reserved.

**Keywords:** Mesoporous silica; Poly(lactide-co-glycolide); Antibiotic; Scaffold; Controlled release

## 1. Introduction

Since the beginning of the 1970s, controlled release technology has experienced great advancement, and motivated more researchers in materials science, chemistry and bio-

medicine to exert great efforts to develop controlled release systems for different applications [1]. Controlled release systems overcome the disadvantage of traditional drug dosage form, and offer more effective and favorable methods to optimize drug dosage, deliver to specific sites or prolong delivery duration [2]. Nanoparticles [3], mesoporous materials [4], and lipids [5] are the more familiar carriers for delivering genes [6], drugs [7–9] and growth factors [10].

Mesoporous materials, which contain pores with diameter between 2 and 50 nm, have been investigated as a drug

\* Corresponding authors. Tel.: +65 6316 8890; fax: +65 67911761.

E-mail addresses: [imwangyj@scut.edu.cn](mailto:imwangyj@scut.edu.cn) (Y.J. Wang), [DAWang@ntu.edu.sg](mailto:DAWang@ntu.edu.sg) (D.-A. Wang).

<sup>1</sup> These authors contributed equally to this paper.

delivery system since the 1980s [11]. At present, they have been extensively applied in various fields, such as separation [12], catalysis [13], adsorption [14], sensor [15], and photonics [16]. A new application of mesoporous silica – the confinement of a drug or gene in the pores of the material for controlled delivery – was first proposed in 2001 [17], and a wide range of drugs carriers using these kinds of materials have been developed [18,19]. Mesoporous materials have highly organized porous structure with uniform pore size and vast surface area, which make them an excellent candidate as a release carrier.

At present, the most common antibiotic carrier to treat infection after the removal of necrotic bone tissue induced by chronic bacterial osteomyelitis is poly(methylmethacrylate) (PMMA) beads [20–22]. However, these systems must be removed in a second surgical procedure [2]. Herein, we developed new multifunctional composite materials which were produced by hybridizing HMS–HA and PLGA. Gentamycin sulfate (GS), a model antibiotics, was loaded into the HMS–HA particles and then embedded by PLGA spheres for controlled release [23]. Microspheres sintering technique [24,25] was employed to fabricate the PLGA/HMS–HA microspheres scaffold. As a potential drug delivery carrier which can also be used as bone repair material, HMS–HA has the high bioactivity of HA and also inherits the mesoporous structure of HMS. Bioactivity evaluation of the material was done to illuminate its safety and its potential in promoting bone regeneration. HMS–HA particles were used to improve the mechanical properties of PLGA scaffolds, to compensate for the decreased pH values induced by the acidic degradation products of PLGA and to enhance the viability of cells on the scaffolds. On the other hand, PLGA plays an important role in the bonding of HMS–HA particles in the modified scaffold and makes the drug release time longer.

## 2. Materials and methods

### 2.1. Materials

Tetraethyl orthosilicate (TEOS), ethyl alcohol (EtOH),  $\text{Ca}(\text{NO}_3)_2$ ,  $(\text{NH}_4)_2\text{HPO}_4$  and methylene chloride were purchased from Chemical Reagent Factory (Guangzhou, China). Dodecylamine (DDA) was supplied by SSS Reagent (Shanghai, China). Poly(lactic-co-glycolic acid) with a ratio of lactic to glycolic acid monomer units of 50:50 was purchased from Daigang Biomaterials (Jinan, China). This copolymer has an average molecular weight of  $31,000 \text{ g mol}^{-1}$  with an inherent viscosity of  $0.30 \text{ dl g}^{-1}$  in chloroform at  $30^\circ\text{C}$ . Gentamycin sulfate (GS) was purchased from Probe (Beijing, China). Poly(vinyl alcohol) (PVA) was obtained from Sigma–Aldrich (Singapore).

### 2.2. Preparation of HMS–HA–GS composite particles

HMS–HA was synthesized following the method described in Ref. [26]. Briefly, DDA was dissolved in

EtOH/deionized water solution (pH 9) containing  $\text{Ca}(\text{NO}_3)_2$ ,  $(\text{NH}_4)_2\text{HPO}_4$  and  $\text{NH}_4\text{OH}$ . Subsequently, TEOS was added as a silica source and the mixture was stirred at 200 rpm. The reaction mixture conformed to the following molar composition: TEOS: 1.0, DDA: 0.27, EtOH: 9.09,  $\text{H}_2\text{O}$ : 29.6,  $\text{Ca}(\text{NO}_3)_2$ :1.0,  $(\text{NH}_4)_2\text{HPO}_4$ : 0.6. The mixture was stirred for 1 h, and then aged for 18 h at room temperature. The product was dried at  $90^\circ\text{C}$ , and then the DDA template was removed by EtOH extraction. The nitrogen adsorption/desorption, surface area, and median pore diameter of HMS–HA were measured using a Micromeritics ASAP 2010 M sorptometer.

The HMS–HA–GS particles were achieved by pouring 150 mg dried HMS–HA particles into  $100 \text{ mg ml}^{-1}$  GS solution. The HMS–HA particles were then soaked in the GS solution for 5 days at  $4^\circ\text{C}$  followed by filtration and drying at  $37^\circ\text{C}$ . The drug-loaded silica particles were weighed again to determine the amount of the loaded drug.

### 2.3. Fabrication of PLGA microspheres, PLGA/HMS–HA microspheres, and PLGA and PLGA/HMS–HA microspheres sintered scaffolds

PLGA microspheres were prepared using a double emulsion solvent evaporation technique (water/oil/water). GS was dissolved in sodium phosphate buffer (pH 7.2) as the first water phase. Five grams of PLGA was dissolved in 25 ml methylene chloride while the mixture was stirred as the oil phase, and then the first water phase and oil phase were homogenized at 5000 rpm for 30 s with a homogenizer. The emulsion was added dropwise to a 0.5% PVA aqueous solution, and the mixture was stirred for 4 h at 200 rpm, allowing the complete evaporation of the solvent. PLGA microspheres were isolated by vacuum filtration, and washed five times with deionized water.

PLGA/HMS–HA–GS microspheres were prepared using a single emulsion solvent evaporation method. Briefly, 5 g PLGA and HMS–HA–GS particles (1 or 2.5 g) were dissolved in 25 ml methylene chloride, and the mixture was sonicated for 1 min. The resultant mixture was then poured into a 0.5% PVA aqueous solution and stirred for 8 h. PLGA/HMS–HA–GS microspheres were isolated and washed five times with deionized water.

PLGA or PLGA/HMS–HA–GS microsphere sintered scaffolds were fabricated by pouring PLGA microspheres or PLGA/HMS–HA–GS microspheres into cylindrical molds, and then were sintered at  $70^\circ\text{C}$  for 2 h.

### 2.4. GS encapsulation efficiency of HMS–HA particles and PLGA/HMS–HA microspheres

#### 2.4.1. GS encapsulation efficiency of PLGA/HMS–HA microspheres

Fifty micrograms of PLGA/HMS–HA microspheres were dissolved in 3 ml methylene chloride and centrifuged. The upper solution was collected, leaving out a lower deposit layer. The above process was repeated five times.

A: The upper solution was mixed with 2.5 ml PBS solution. The mixture was stirred for half an hour in order to release all the GS into the aqueous phase. The GS content in the PBS solution was analyzed by a UV spectrophotometer at 333 nm wavelength using the method described in Ref. [27].

B: The deposit (bottom layer) was considered to be pure HMS–HA particles free of PLGA. The solid layer was mixed with 10 ml PBS, and placed at 37 °C for 24 h. The GS content was determined by a UV spectrophotometer.

The GS encapsulation efficiency of PLGA/HMS–HA was determined by the equation as follows:

$$\text{Encapsulation efficiency} = (C_t + C_b)/C_p \quad (1)$$

where  $C_t$  and  $C_b$  are the GS content of the upper and bottom layers described above.  $C_p$  denotes the GS content in the HMS–HA before blending with PLGA, respectively.

### 2.5. In vitro studies in SBF

Biomineralization studies in vitro were conducted to evaluate bioactivity of HMS–HA. Simulated body fluid (SBF) was prepared according to Kokubo's recipe [28] (Table 1). HMS–HA particles (100 mg) were laid down in the SBF system (200 ml) at 37 °C, and taken out of SBF at regular time intervals. The products were rinsed with distilled water and dried at 37 °C. All the samples were stored at 4 °C for further use. The decrease of Ca and P concentration in SBF solution, which is indicative of calcium phosphate formation, was followed by the methods described in the Refs. [29–31].

### 2.6. In vitro release test for GS from HMS–HA particles and sintered microspheres scaffolds

Gentamicin release in vitro was determined by suspending HMS–HA particles (100 mg) or PLGA/HMS-based microspheres (150 mg) in 20 ml PBS buffer (pH 7.4) at 37 °C. The release media were collected at regular time intervals with equal amount of PBS makeup. All samples of release media were stored at 4 °C prior to analysis of GS concentration.

### 2.7. SEM analysis

HMS–HA particles before and after the process of biomineralization, and the morphology of PLGA–GS microspheres and PLGA/HMS–HA–GS microspheres, were characterized by a scanning electron microscopy (SEM). The energy dispersive X-ray spectrometer (EDX)

(30XLFEQ, Philips, The Netherlands) was used to analyze element content of HMS–HA.

### 2.8. Degradation studies

Cylindrical PLGA, PLGA/HMS–HA (20%), and PLGA/HMS–HA (50%) scaffolds (diameter = 10 mm) were weighed and then soaked in bottles filled with 10 ml phosphate buffered saline (PBS) solution (pH 7.2). All the bottles were incubated at 37 °C. The weight and pH values were measured every 10 days. Weight loss was calculated using the following equation:

$$\text{Weight loss}(\%) = 100 \times (M_{t/\text{wet}} - M_{t/\text{dry}})/M_0 \quad (2)$$

where  $M_0$  and  $M_t$  are the initial mass and the mass after  $t$  day's immersion, respectively.

### 2.9. Porosity determination of scaffolds

Ethanol was used as the liquid phase and kept at 25 °C. A bottle filled with ethanol was weighed ( $W_1$ ). Then a scaffold sample (cylindrical scaffolds, diameter = 10 mm, height = 20 mm) weighing  $W_s$  was immersed into the bottle and weighed ( $W_2$ ).  $\rho$  is the density of ethanol at 25 °C. The size of the cylindrical scaffold including radius ( $R$ ) and height ( $H$ ) was measured. The porosity ( $P$ ) was calculated using the equations as follows:

$$P = 1 - ((W_1 - W_2 + W_s)/\rho)/((\pi \times R^2) \times H) \quad (3)$$

### 2.10. Mechanical behavior test

The compressive strength and compressive modulus of the cylindrical scaffolds (diameter = 10 mm, height = 20 mm) was measured using a universal material testing machine (Instron 5567, Instron Corp., USA) at a crosshead speed of 5 mm min<sup>-1</sup> for compressive strength tests and 50 mm min<sup>-1</sup> for DTS tests.

### 2.11. Cell culture

Porcine mesenchymal stem cells were harvested using the method described in Ref. [32] and were propagated in Dulbecco's modified Eagle's medium (DMEM) with supplements of 1.5 mg ml<sup>-1</sup> sodium bicarbonate, 4.5 mg ml<sup>-1</sup> glucose, 10% (v/v) fetal bovine serum (FBS), 100 U ml<sup>-1</sup> penicillin, and 100 µg ml<sup>-1</sup> streptomycin. All the reagents above were purchased from Gibco (Invitrogen, Singapore). The fabricated scaffolds were sterilized by 70% ethanol for 2 h followed by PBS wash. All the scaffolds were pre-wetted in the culture medium for 12 h.

### 2.12. Cell toxicity evaluation

Cell proliferation was measured using the WST-1 reagent (Roche Diagnostics, Germany), which relied upon the ability of living cells to reduce a tetrazolium salt into a

Table 1  
Ion concentration of SBF.

	Ion concentration							
	Na <sup>+</sup>	K <sup>+</sup>	Ca <sup>2+</sup>	Mg <sup>2+</sup>	Cl <sup>-</sup>	HCO <sub>3</sub> <sup>-</sup>	HPO <sub>4</sub> <sup>2-</sup>	SO <sub>4</sub> <sup>2-</sup>
SBF	142.0	5.0	2.5	1.5	147.8	4.2	1.0	0.5

soluble colored formazan product. Cell suspensions (5000 cells/well) were seeded into a 24-well cell culture plate and grown overnight. Different microspheres scaffolds (PLGA and PLGA/HMS–HA) were placed into each well, and the tissue culture plates (TCP) without scaffolds were used as control. After treatment of the cells with scaffolds for 3, 5 and 7 days, the supernatant medium was replaced by WST-1 diluted 1:20 (v/v) with DMEM and incubated for 3 h. Analyses were performed in triplicates. The absorbance in each well was measured using a microplate reader set to 450 nm with a reference wavelength of 625 nm.

### 2.13. Cell seeding and proliferation on the scaffolds

Fifty microlitres of cells in suspension ( $1 \times 10^8$  cells  $\text{ml}^{-1}$ ) were seeded on every scaffold. The cells were allowed to adhere to the scaffolds for 3 h, and 750  $\mu\text{l}$  of culture medium was added to each scaffold. The cell–scaffolds complexes were placed at 37 °C in a humidified incubator of 5%  $\text{CO}_2$  for 14 days. Cell numbers on the scaffolds was determined by DNA quantitation kit (Sigma, Singapore). The cell numbers were calculated from a DNA standard curve of identical cells. Cell viability on the scaffolds was detected on day 14 using a “Live/Dead” assay (Molecular Probes, Invitrogen, Singapore), and only “Live” assay was performed in this study.

### 2.14. Statistical analysis

Experiments were repeated three times and results were expressed as means  $\pm$  standard deviations. Statistical sig-

nificance was calculated using one-way analysis of variance (one-way ANOVA). Comparison between the two means was determined using the Tukey test and statistical significance was defined as  $p < 0.05$ .

## 3. Results and discussion

HMS–HA is a newly developed material, which inherits high surface areas produced by nanopores from HMS. Besides, it may also render good bioactivity from HA and biocompatibility from silica. Compared with nanoparticles, the special mesoporous structure which supplies space to host large amount of drug molecules makes HMS–HA predominantly suitable for drug delivery. In this study, apatite nucleation in the pores of HMS adopted a self-assembly technique in situ [26]. HMS was chosen as the silica matrix because the template removal route is very simple and only requires a low temperature (below 100 °C). The low temperature for template removal facilitates the regulation of the HA crystallinity in HMS matrix.

### 3.1. Preparation of HMS–HA

Fig. 1 shows the structure of HMS and HMS–HA. DDA (containing  $\text{Ca}(\text{NO}_3)_2$  and  $(\text{NH}_4)_2\text{HPO}_4$ ) was utilized as a template to form the sheet structure in EtOH solution. TEOS self-assembles on the surface of DDA sheet structure through hydrogen bonding between the electron lone pairs on the nitrogen of the surfactant and the proton on hydroxyl group of the silanol precursor [26]. At the same time,  $\text{Ca}^{2+}$  and  $\text{PO}_4^{3-}$ , which are enveloped by

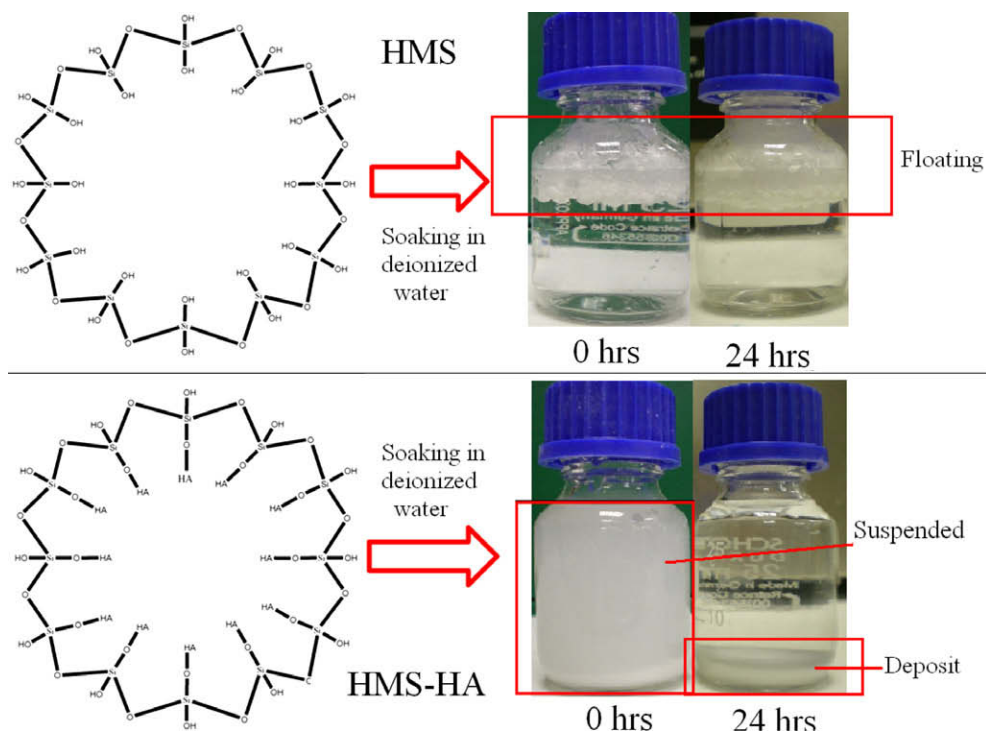


Fig. 1. Molecular structures of HMS and HMS–HA. HMS and HMS–HA was added to water solution and kept for 24 h, and the distribution state of particles was recorded by camera.

TEOS, react at appropriate pH value (pH 9), and finally form hydroxyapatite. The template was removed via washing by hot EtOH, and HA crystals grew simultaneously. Template removal produces a mass of silicate hydroxyl exposed on the pore wall of HMS. The interaction between silicate hydroxyl of HMS and the hydroxyl of HA enables HA crystals to coalesce with mesoporous silica and to form uniformly stepwise monolayer in the pores of HMS [26].

The distribution property in aqueous solution of HMS–HA and HMS particles was also demonstrated in Fig. 1. We found that HMS–HA particles could be suspended in deionized water uniformly with gentle shaking. By contrast, most of the HMS particles float on the deionized water in the beginning even after adequate vortex. After being soaked in deionized water for 24 h, most of HMS–HA particles get deposited at the bottom of the bottle. However, HMS particles still float on the deionized water. The surface tension between inorganic particles and water might explain this phenomenon. After the introduction of HA into the mesoporous silica, particles became more hydrophilic. HMS–HA has good distribution ability in water phase, and this special characteristic benefits HMS–HA as a potential drug delivery vehicle. Before the introduction of HA, most of the HMS particles have pore size less than 1 nm, which may limit their utility as a carrier for drugs or proteins with large molecular structures. The assembly and growth of HA into the pores of HMS can enlarge the pore size to about 3.3 nm (Table 2) [26]. It is very difficult to make HMS particles uniformly distributed in aqueous solution. Thus, the particles do not come into sufficient contact with water-soluble drugs. After the introduction of HA, the HMS–HA particles became more hydrophilic and exhibit good distribution property in aqueous solution as described above, which favors HMS–HA particles as a better release vehicle for hydrophilic drugs. These two advantages make the HMS–HA particles more suitable for drug loading.

### 3.2. Biomineralization of HMS–HA in SBF

The biomineralization of HMS–HA particles in vitro was examined in SBF solution. Inorganic biomaterials such as bioactive glass and hydroxyapatite have demonstrated the ability of living bone binding. The basic characteristic of these materials is to form a layer of bone-like apatite on their surface after incubation in the simulated body fluid

(SBF), the ion concentrations of which are homologous with human blood plasma [27]. Therefore, bioactivity of bone tissue engineering materials in vivo can be predicted from the apatite formation ability on their surface in SBF [27].

As shown in Fig. 2, calcium and phosphorus, the main elements of apatite, were not found on the surface of HMS after it was soaked in SBF solution for 7 days. On the contrary, HMS–HA exhibited great capacity to induce the bone-like apatite deposition. The surface state of HMS–HA before and after mineralization is also shown in Fig. 2. Irregular sheet-shaped smooth surface of HMS–HA became rough, and at the same time, small pieces of HMS–HA coalesced into large agglomerations after being soaked in SBF solution for 3 days. On Day 7, the sizes of the agglomerations became larger, and fuzz-like apatite deposited on the surface.

EDX was used to obtain the values for Ca/P ratio and (Ca + P)/Si ratio (Fig. 2 and Table 3). Theoretical values of Ca/P and (Ca + P)/Si ratios of HMS–HA before mineralization were 1.67 and 0.4, respectively, which were calculated based on the original reagents used for HMS–HA synthesis. The actual values of synthesized HMS–HA were almost identical to the theoretical values (1.60 and 0.39). After mineralization for 3 days and 7 days, the ratios of Ca/P and (Ca + P)/Si were 1.40 and 0.49, and 1.44 and 0.79, respectively. Compared with HMS–HA before mineralization, the (Ca + P)/Si values of the HMS–HA after mineralization increased remarkably. On the other hand, the (Ca + P)/Si ratio increased with the increase of exposure time in SBF, which may be due to more apatite deposition on the HMS–HA surface. The new apatite formation of HMS–HA was also confirmed by the results of Ca and P concentration variation in SBF (Fig. 3). The Ca and P concentration significantly decreased in SBF solution at Day 14 for HMS–HA. However, there was almost no change of Ca and P concentration as HMS is soaked in SBF solution.

### 3.3. HMS–HA particles for GS delivery

Table 2 exhibited the surface area and median pore diameter of HMS–HA inorganic particles. HMS–HA has vast surface area ( $332 \text{ m}^2 \text{ g}^{-1}$ ), and the mesopores in HMS–HA particles (the median diameter = 3.3 nm) are enough for encapsulating GS molecules.

The release kinetics of GS from HMS–HA particles as a function of contact time in PBS solution are plotted in Fig. 4. Around 60% of GS molecules were released into PBS solution in the first hour. In the subsequent 11 h, remarkably low release rate was exhibited in comparison with the first hour. GS molecules hosting in the mesopores could be divided into two parts in drug delivery kinetics. Some GS molecules get absorbed on the external surface of matrix or distributed around the location close to mesopores. The GS molecules which interact with HMS–HA by physical absorption might be released

Table 2  
Porosity, surface area and median pore diameter of HMS–HA particles [26] and PLGA/HMS–HA scaffolds.

Batch	Porosity (%)	Surface areas ( $\text{m}^2 \text{ g}^{-1}$ )	Median pore diameter
HMS–HA	–	332	3.3 nm
PLGA/20% HMS–HA scaffold	$37.2 \pm 3.7$	–	$(122 \pm 11) \mu\text{m}$
PLGA/50% HMS–HA scaffold	$40.2 \pm 4.9$	–	$(115 \pm 16) \mu\text{m}$

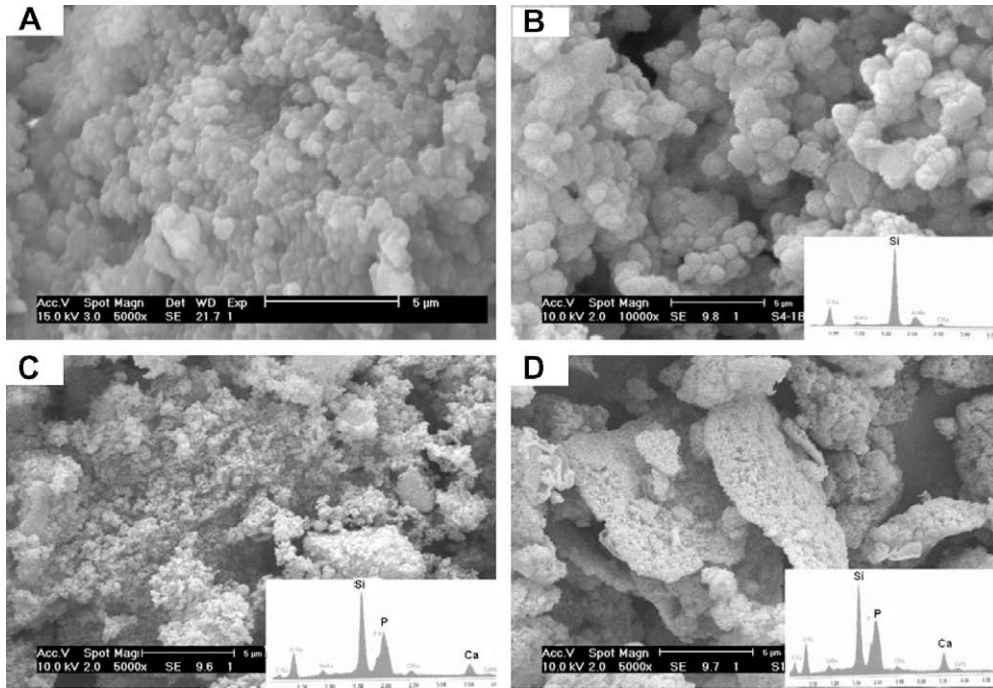


Fig. 2. SEM and inserted EDX images of HMS–HA particles (A), and HMS soaked in SBF solution for 7 days (B), apatite formation on HMS–HA in SBF after day 3 (C) and day 7 (D).

Table 3  
Ca/P and (Ca+P)/Si ratio of HMS–HA before and after biomineralization.

Sample	HMS–HA (T)	HMS–HA (A)	HMS–HA –D3	HMS–HA –D7
Ca/P	1.67	1.60	1.40	1.44
(Ca+P)/Si	0.40	0.39	0.49	0.79

T, theoretical values; A, actual values.

quickly, inducing the initial burst release. The rest of the GS which interacts with silanols of HMS and hydroxyl of HA and forms hydrogen bonds might get released slowly.

A two-step release model proposed by Andersson which was based on Higuchi model was applied to inves-

tigate the GS release behavior from HMS–HA [33,34]. Based on Fick’s law, the equation of Higuchi model used to predict drug release rates from a porous carrier matrix is:

$$M_{\infty} = Kt^{1/2} / 2M_t / M_{\infty} = Kt^{1/2} \quad (4)$$

$M_t$  is the drug released at time  $t$ ,  $M_{\infty}$  is the quantity of drug released at infinite time, and  $K$  is the kinetic constant.  $K$  as the kinetic release constant is determined by the diffusivity of the drug in the solvent, the porosity of the matrix, the total amount of drug present in the matrix and the solubility of the drug in the solvent used. The GS release from HMS–HA (Fig. 4) is divided into two processes: a fast initial burst release followed by a second stage of slower release, and the transitional inflexion at around Days 1–2.

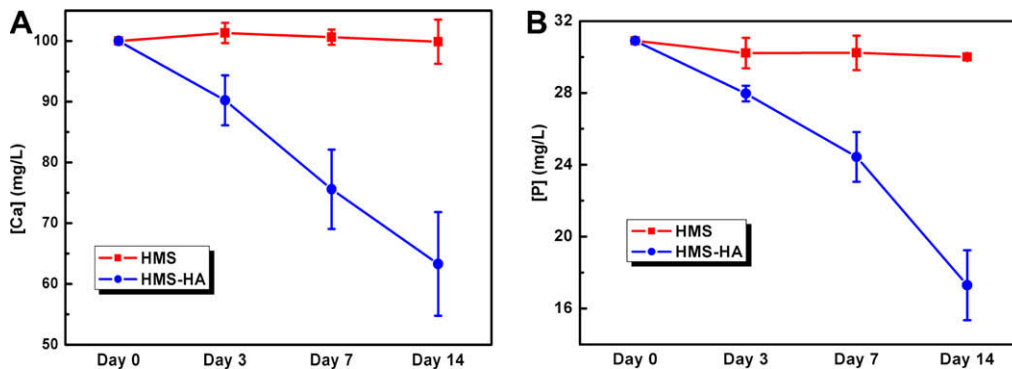


Fig. 3. Calcium (A) and phosphorus (B) concentration in SBF at 3, 7, and 14 days for HMS and HMS–HA.

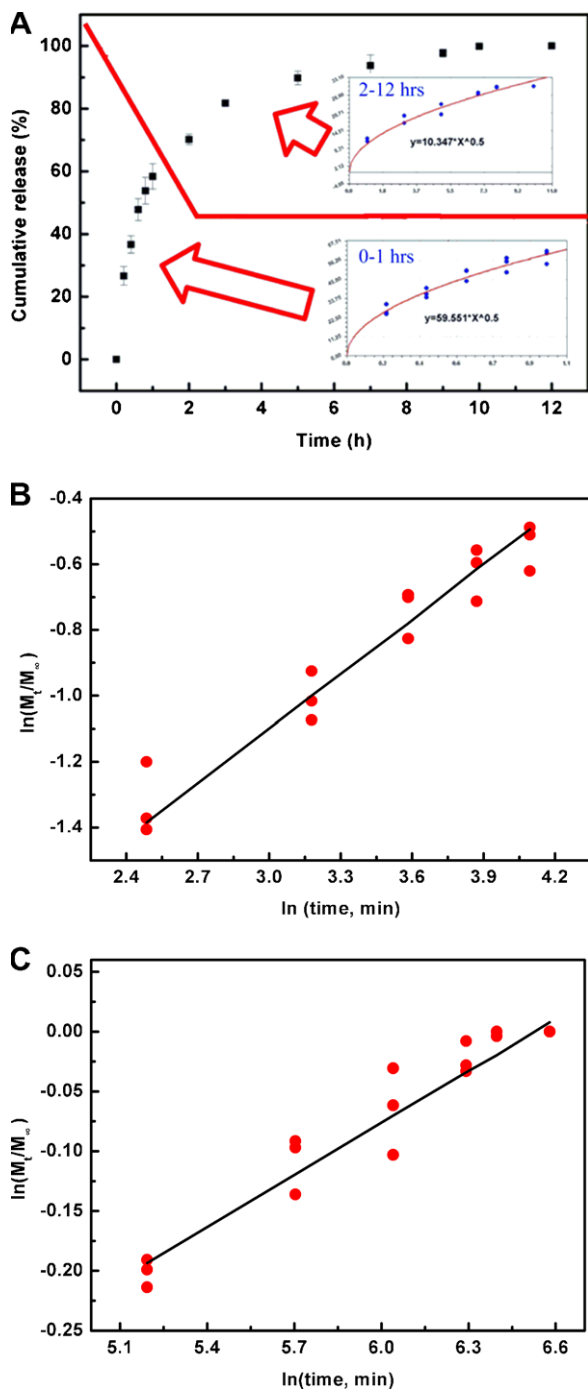


Fig. 4. Cumulative release profiles of GS from HMS-HA particles (A), and the plots of the logarithm of GS released from HMS-HA as a function of the logarithm of time according to the Higuchi model (B, 0–1 h and C, 2–12 h).

The first release step may be due to the release of drug molecules diffusing out of mesopores, and the second step can be attributed to the release of GS molecules entrapped into the channel of mesoporous silica-apatite composite particles. Both of the kinetics curves of these two processes exhibit good linearity ( $r^2 > 0.98$ ) (Fig. 4B and C), which indicates that drug diffusion and release from HMS-HA corresponds to Fick's law.

### 3.4. Characteristic of PLGA/HMS-HA scaffolds

The 3-D bone tissue engineering scaffold with controlled drug release function was fabricated via PLGA microspheres sintering technique. The morphology of PLGA/HMS-HA-GS sintered microspheres scaffolds is exhibited in Fig. 5. The SEM images indicate that the inorganic-organic composite microspheres possess a round structure with rough surface. The bond areas can be found among the microspheres, which are induced by the action of sintering.

The HMS-HA confirmed to its function of pH-compensation as described earlier. As shown in Fig. 6A, compared with pure PLGA scaffold, blending 50% HMS-HA with PLGA increased the pH value from 5.0 to 6.5 on day 60, which might effectively reduce inflammatory responses induced by pH value decrease in clinical applications. The degradation of PLGA is a process in which ester bonds get hydrolyzed into lactic and glycolic acid, and a mass of acidic degradation products get released resulting in remarkable decrease in the pH value of the surroundings. Hydroxyapatite balances the pH values during the degradation process. Fig. 6B demonstrates the weight loss of the PLGA microspheres scaffolds with different HMS-HA content during the degradation process. No significant difference was observed between PLGA and PLGA/HMS-HA scaffolds in weight loss during the first month. However, after 60 days, PLGA had a faster degradation ratio than other types of scaffolds with HMS-HA particles. This result might be due to the non-degradable characteristic of HMS and the HA-induced pH neutralization reaction which postpones the degradation process of PLGA/HMS-HA.

Fig. 7 demonstrates the compressive strength and the compressive modulus of the PLGA/HMS-HA-GS and PLGA double emulsion scaffolds. As a result of double emulsion solvent evaporation fabrication process, the interior of the PLGA double emulsion microspheres maintained large amount of porous structures [35], which decreased the mechanical properties of PLGA scaffolds. Compared with PLGA scaffolds, PLGA/HMS-HA-GS scaffolds show high compressive strength and compressive modulus. The compressive strength and compressive modulus of PLGA/20% HMS-HA, PLGA/50% HMS-HA scaffolds are 5.44 and 158.12, and 8.33 and 215.32 MPa, respectively. While on the contrary, the compressive strength and compressive modulus of PLGA scaffolds are only 0.5 and 1.27 MPa, respectively.

One challenging problem in the field of bone tissue engineering is to achieve the balance of mechanical properties between the load-bearing site and the tissue regeneration scaffolds. An ideal strength which is equal to bone tissue for load-bearing purposes requires that the scaffolds have minimal porosity. By contrast, cells attachment, proliferation, and vascularization require the scaffolds to have high porosity and appropriate pore size. Therefore, an ideal scaffold should not only have enough mechanical proper-

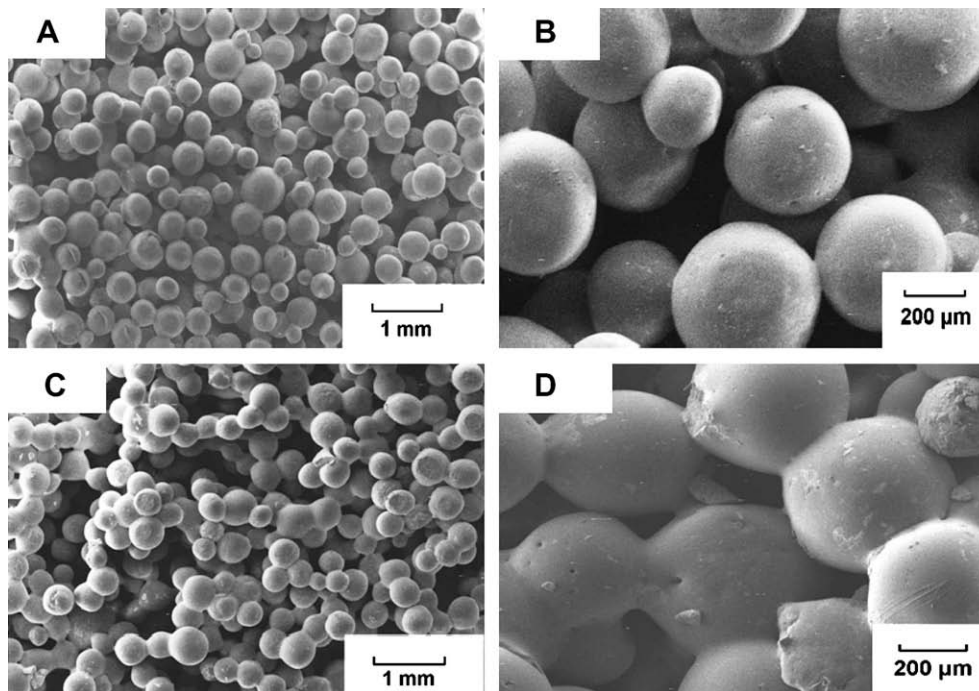


Fig. 5. SEM images of PLGA/HMS-HA-GS (20wt.%) (A and B) and PLGA/HMS-HA-GS (50wt.%) (C and D) sintered microspheres scaffolds.

ties to resist the physiological mechanical environment at an implantation site, but also favor cell growth and nutrition exchange. The conventional PLGA porous scaffolds fabricated via solvent casting/particulate leaching and thermally induced phase separation have low mechanical performance. In this study, the microspheres sintering technique for scaffolds fabrication developed by Borden and Laurencin was applied [36]. The porosity and median pore diameter of PLGA/20% HMS-HA and PLGA/50% HMS-HA scaffolds are  $(37.2 \pm 3.7)\%$  and  $(40.2 \pm 4.9)\%$ , and  $(132 \pm 11) \mu\text{m}$  and  $(115 \pm 16) \mu\text{m}$ , respectively. And microsphere sintered scaffolds with similar structure have been confirmed to be able to facilitate cell ingrowth and proliferation [24]. The compressive modulus and compressive strength of them are around 100–250 and 4–10 MPa, respectively, which approach the mechanical properties of cancellous bone (Compressive strength is 50–500 MPa and compressive modulus is 2–12 MPa) [37].

### 3.5. PLGA/HMS-HA scaffolds for GS release

Table 4 shows the GS loading efficiency of PLGA/HMS-HA. During the double emulsion process for microspheres fabrication, 49.8% and 40.1% GS was lost, and the final GS loading of PLGA/HMS-HA (20%) and PLGA/HMS-HA (50%) was 51.2% and 59.9%, respectively.

The release of GS in vitro from PLGA/HMS-HA scaffolds was performed under the same experimental conditions and at the same time points. As shown in Fig. 8, there was little difference in the release profiles between PLGA microspheres with 20wt.% and 50wt.% HMS-HA

content. A remarkable burst release was observed during the first two hours, and almost 60% GS was released into PBS solution. Subsequently, a low dose of GS was released from both types of scaffolds, and the whole release process lasted for 30 days. GS molecules in the PLGA/HMS-HA scaffold could be said to be released in two stages. At the first stage, the GS molecules which were attached to the external surface of microspheres or HMS-HA particles induced a burst release. PLGA/50% HMS-HA exhibited higher release rate than that of PLGA/20% HMS-HA. During the second stage, the GS molecules that were bound to HMS-HA through hydrogen bonds, and the HMS-HA particles that were wrapped by PLGA both led to low GS release rate. PLGA plays an important role in this stage. It blocks the main passage of drug delivery on the HMS surface, and acts as an envelope enclosing HMS particles. After 30 days of release, almost all of the GS molecules were released into the PBS solution. The modified method of using PLGA in the second phase to control GS release achieved remarkable influence for delaying drug release into solution. The release time prolonged from around 12 h of HMS-HA particles to almost one month for PLGA/HMS-HA.

### 3.6. Cell toxicity evaluation

Cell toxicity of the scaffolds was analyzed using WST-1 assay after 3, 5 and 7 days of culture. WST-1 assay analyzes the viability of cells by measuring the activity of mitochondrial dehydrogenases. As shown in Fig. 9A, an increase in absorbance from Day 3 to Day 7 was recorded,

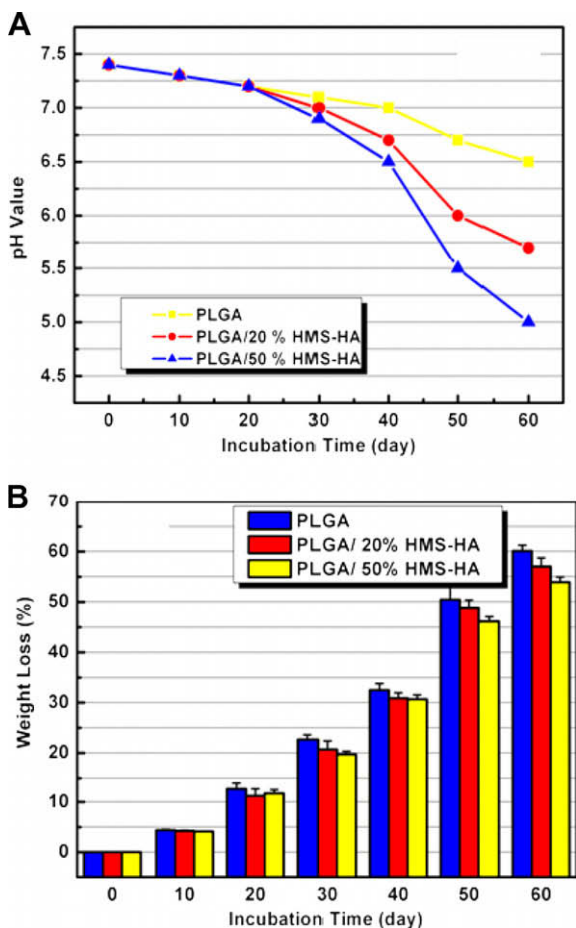


Fig. 6. (A) pH value variation of PBS solution during the degradation of PLGA-GS and PLGA/HMS-HA-GS scaffolds. (B) Weight losses for PLGA-GS and PLGA/HMS-HA-GS scaffolds during the degradation process.

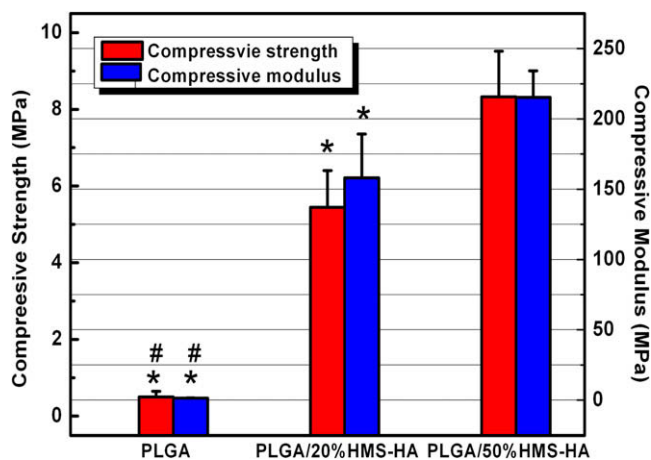


Fig. 7. Mechanical properties evaluation in compression for PLGA-GS and PLGA/HMS-HA-GS scaffolds. (#) and (\*) indicate statistical significance when compared with PLGA/20% HMS-HA-GS and PLGA/50% HMS-HA-GS scaffolds ( $p < 0.05$ ) (red bar: compressive strength; blue bar: compressive modulus). (For interpretation of color mentioned in this figure the reader is referred to the web version of the article.)

which indicates that the cells were viable with all the scaffolds. On the third day, the proliferation of cells with PLGA/HMS-HA scaffolds was observed to be significantly higher than that with pure PLGA scaffolds. After 7 days of culture, PLGA/50% HMS-HA exhibited remarkable cell viability, which was nearly 20% and 30% higher than that of PLGA/20% HMS-HA and PLGA scaffolds. As a widely used drug and protein delivery system, the low cell toxicity of PLGA microspheres has already been accepted. The bioactivity of hydroxyapatite with low crystallinity is also undoubted because of the similarity to natural bone mineral. Compared with pure PLGA scaffolds, PLGA/HMS-HA scaffolds exhibit higher cell viability, possibly due to hydroxyapatite with low crystallinity in the mesoporous silica [38].

### 3.7. Cell proliferation on the scaffolds

Porcine mesenchymal stem cells were seeded onto pure PLGA and PLGA/HMS-HA scaffolds over 14 days of culture period in vitro. Cells (500,000) were seeded onto each scaffold, and more than 250,000 cells were attached on each scaffold on the first day. The cell attachment efficiency of pure PLGA, PLGA/20% HMS-HA and PLGA/50% HMS-HA scaffolds were  $(57.83 \pm 8.73)\%$ ,  $(59.24 \pm 15.2)\%$  and  $(68.51 \pm 13.84)\%$ , respectively. After 3 and 7 days of culture, the cell proliferation on the scaffolds exhibited no significant differences among all types of scaffolds. However, on day 14, PLGA/HMS-HA scaffolds showed higher cell proliferation than that of pure PLGA scaffolds

Table 4  
GS loading efficiency of HMS-HA particles and PLGA/HMS-HA scaffolds.

Variables	GS loading in HMS-HA	GS loading in scaffolds (%)
PLGA/20% HMS-HA	(335 ± 70) mg GS / 1000 mg HMS-HA	51.2 ± 3.35
PLGA/50% HMS-HA		59.9 ± 2.16

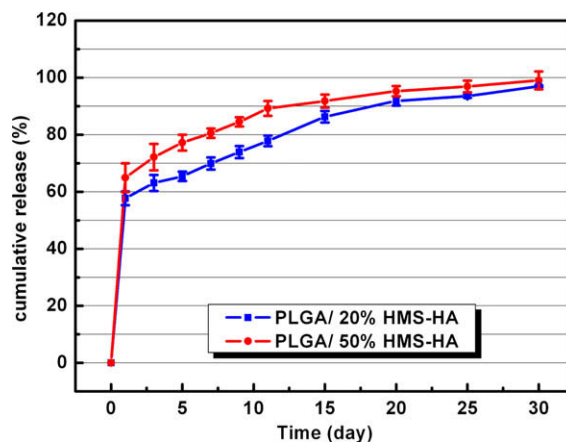


Fig. 8. Cumulative release profiles of GS from PLGA/HMS-HA scaffolds with different HMS-HA content.

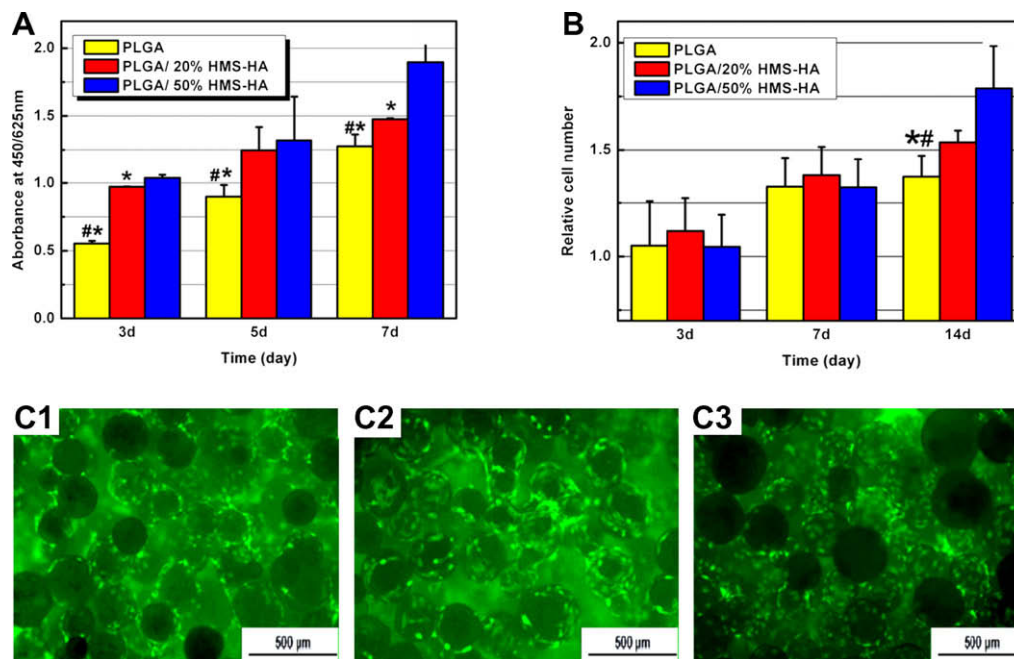


Fig. 9. (A) Cell toxicity evaluation by WST of PLGA scaffold, PLGA/HMS-HA (20wt.% and 50wt.% HMS-HA) scaffolds and control. (#) and (\*) indicate statistical significance when compared with PLGA/20% HMS-HA-GS and PLGA/50% HMS-HA-GS scaffolds ( $p < 0.05$ ). (B) Relative cell proliferation ratios for the PLGA scaffold and PLGA/HMS-HA scaffolds (20wt.% and 50wt.% HMS-HA) on day 3, day 7, and day 14. (#) and (\*) indicate statistical significance when compared with PLGA/20% HMS-HA-GS and PLGA/50% HMS-HA-GS scaffolds ( $p < 0.05$ ). (C) Cells growth on the PLGA scaffold (c1) and PLGA/HMS-HA scaffolds (20wt.% c2 and 50wt.% HMS-HA c3) on day 14.

(Fig. 9b). The fluorescence microscope images (Fig. 9c) showed observable cell viability on the scaffolds. All types of scaffolds with cells were stained by a “live/dead” assay after 14 days of culture in vitro. A dramatically large cell number was observed when cells were cultured on the PLGA/HMS-HA (50%) scaffold, as compared to other types. A more detailed observation of the cells suggested that, for the sintering microspheres scaffolds, cells grew around the gaps among the microspheres. When the gaps were filled or almost filled, the cells would be apt to grow on the surface of the microspheres.

#### 4. Conclusion

As an implantable drug delivery system for local drug delivery/release in bone tissue, HMS-HA exhibits excellent biomineralization ability and controlled drug release properties. The GS release time can last for 12 h, and the drug release curve exhibits good linearity while the release process follows Fick’s law. This novel scaffold based on HMS-HA and PLGA shows similar mechanical properties to human cancellous bone, which lends more support for it becoming a promising candidate for bone tissue regeneration. In addition, PLGA/HMS-HA scaffolds exhibit positive effects on drug delivery and cell proliferation. As a bifunctional scaffold, it may offer more advantages for clinical applications. In future work, we will focus on the osteogenic differentiation of porcine mesenchymal stem cells on the three-dimensional porous PLGA/HMS-HA microspheres sintered scaffolds.

#### Acknowledgements

Xuetao Shi was a China Scholarship Council (CSC) scholarship recipient (2007U33046). This research was supported by National Key Technologies R&D Program (2006BA116B06), National Basic Research Program of China (2005CB623902), National Science Foundation (50732003, 50830101, 50803018), and the Key Projects in the National Science & Technology Pillar Program in the Eleventh Five-year Plan Period (Grant 2006BA116B04), and also supported by Grant ARC 10/06, Ministry of Education, Singapore.

#### References

- [1] Liu Y, Miyoshi H, Nakamura M. Novel drug delivery system of hollow mesoporous silica nanocapsules with thin shells: preparation and fluorescein isothiocyanate (FITC) release kinetics. *Colloid Surf B* 2007;58:180–7.
- [2] Vallet-Regí M, Balas F, Arcos D. Mesoporous materials for drug delivery. *Angew Chem Int Edit* 2007;46:7548–58.
- [3] Shi X, Wang Y, Ren L, Gong Y, Wang D-A. *Pharm Res* 2009;26:442–30.
- [4] Tourné-Péteilh C, Lerner DA, Charnay C, Nicole L, Bégu S, Devoisselle JM. The potential of ordered mesoporous silica for the storage of drugs: the example of a pentapeptide encapsulated in a MSU-Tween 80. *ChemPhysChem* 2003;4:281–6.
- [5] Porter CJH, Wasan KM, Constantinides P. Lipid-based systems for the enhanced delivery of poorly water soluble drugs. *Adv Drug Deliver Rew* 2008;60:615–6.
- [6] Yang Y, Xu Z, Chen S, Gao Y, Gu W, Chen L, et al. Histidylated cationic polyorganophosphazene/DNA self-assembled nanoparticles for gene delivery. *Int J Pharm* 2008;353:277–82.

- [7] Sill TJ, von Recum HA. Electrospinning: applications in drug delivery and tissue engineering. *Biomaterials* 2008;29:1989–2006.
- [8] Hilder TA, Hill JM. Carbon nanotubes as drug delivery nanocapsules. *Curr Appl Phys* 2008;8:258–61.
- [9] Zhang LF, Yang DJ, Chen HC, Sun R, Xu L, Xiong ZC, et al. An ionically crosslinked hydrogel containing vancomycin coating on a porous scaffold for drug delivery and cell culture. *Int J Pharm* 2008;353:74–87.
- [10] Johnson MR, Lee H-J, Bellamkonda RV, Guldberg RE. Sustained release of BMP-2 in a lipid-based vehicle. *Acta Bioamter*. doi:10.1016/j.actbio.2008.09.001.
- [11] Corma A. From microporous to mesoporous molecular sieve materials and their use in catalysis. *Chem Rev* 1997;97:2373–419.
- [12] Sakamoto Y, Nagata K, Yogo K, Yamada K. Preparation and CO<sub>2</sub> separation properties of amine-modified mesoporous silica membranes. *Micropor Mesopor Mat* 2007;101:303–11.
- [13] Conesa TD, Mokaya R, Yang Z, Luque R, Campelo JM, Romero AA. Novel mesoporous silicoaluminophosphates as highly active and selective materials in the Beckmann rearrangement of cyclohexanone and cyclododecanone oximes. *J Catal* 2007;252:1–10.
- [14] Baccile N, Babonneau F. Organo-modified mesoporous silicas for organic pollutant removal in water: solid-state NMR study of the organic/silica interactions. *Micropor Mesopor Mat* 2008;110:534–42.
- [15] Dai ZH, Ni J, Huang XH, Lu GF, Bao JC. Direct electrochemistry of glucose oxidase immobilized on a hexagonal mesoporous silica-MCM-41 matrix. *Bioelectrochemistry* 2007;70:250–6.
- [16] Gulians VV, Carreon MA, Lin YS. Ordered mesoporous and macroporous inorganic films and membranes. *J Membrane Sci* 2004;235:53–72.
- [17] Vallet-Regi M, Rámila A, del Real RP, Pérez-Pariente J. A new property of MCM-41: drug delivery system. *Chem Mater* 2001;13:308–11.
- [18] Tozuka Y, Oguchi T, Yamamoto K. Adsorption and entrapment of salicylamide molecules into the mesoporous structure of folded sheets mesoporous material (FSM-16). *Pharm Res* 2003;20:926–30.
- [19] Heikkilä T, Salonen J, Tuura J, Hamd MS, Mul G, Kumar N, et al. Mesoporous silica material TUD-1 as a drug delivery system. *Int J Pharm* 2007;331:133–8.
- [20] Vallo CI, Abraham GA, Cuadrado TR, San Román J. Influence of cross-linked PMMA beads on the mechanical behavior of self-curing acrylic cements. *J Biomed Mater Res B* 2004;70:407–16.
- [21] Habraken WJEM, Wolke JGC, Mikos AG, Jansen JA. PLGA microsphere/calcium phosphate cement composites for tissue engineering: in vitro release and degradation characteristics. *J Biomat Sci Polym E* 2008;19:1171–88.
- [22] Habraken WJEM, Wolke JGC, Mikos AG, Jansen JA. Injectable PLGA microsphere/calcium phosphate cements: physical properties and degradation characteristics. *J Biomat Sci Polym E* 2008;17:1057–74.
- [23] Xue JM, Shi M. PLGA/mesoporous silica hybrid structure for controlled drug release. *J Control Release* 2004;98:209–17.
- [24] Jabbarzadeh E, Jiang T, Deng M, Nair LS, Khan YM, Laurencin CT. Human endothelial cell growth and phenotypic expression on three dimensional poly(lactide-co-glycolide) sintered microsphere scaffolds for bone tissue engineering. *Biotechnol Bioeng* 2007;98:1094–102.
- [25] Cushnie EK, Khan YM, Laurencin CT. Amorphous hydroxyapatite-sintered polymeric scaffolds for bone tissue regeneration: physical characterization studies. *J Biomed Mater Res A* 2008;84:54–62.
- [26] Shi X, Wang Y, Wei K, Ren L, Lai C. Self-assembly of nanohydroxyapatite in mesoporous silica. *J Mater Sci-Mater M* 2008;19:2933–40.
- [27] Zhang X, Wyss UP, Pichora D, Goosen MFA. Biodegradable controlled antibiotic release devices for osteomyelitis: optimization of release properties. *J Pharm Pharmacol* 1994;46:718–24.
- [28] Kokubo T, Takadama H. How useful is SBF in predicting in vivo bone bioactivity? *Biomaterials* 2006;27:2907–15.
- [29] Lehtola MJ, Miettinen IT, Vartiainen T, Rantakokko P, Hirvonen A, Martikainen PJ. Impact of UV disinfection on microbially available phosphorus, organic carbon, and microbial growth in drinking water. *Water Res* 2003;37:1064–70.
- [30] Finish Standards Association. Determination of total phosphorus in water, digestion with peroxodisulfate. SFS 3026. Helsinki: Finish Standards Association SFS, 1986.
- [31] Gregory CA, Gunn WG, Peister A, Prockop DJ. An alizarin red-based assay of mineralization by adherent cells in culture: comparison with cetylpyridinium chloride extraction. *Anal Biochem* 2004;329:77–84.
- [32] Yokoyama A, Sekiya I, Miyazaki K, Ichinose S, Hata Y, Muneta T. In vitro cartilage formation of composites of synovium-derived mesenchymal stem cells with collagen gel. *Cell Tissue Res* 2005;322:289–98.
- [33] Qu F, Zhu G, Lin H, Sun J, Zhang D, Li S, et al. Drug self-templated synthesis of ibuprofen/mesoporous silica for sustained release. *Eur J Inorg Chem* 2006;19:3943–7.
- [34] Andersson J, Rosenholm J, Areva S, Lindn M. Influences of material characteristics on ibuprofen drug loading and release profiles from ordered micro- and mesoporous silica matrices. *Chem Mater* 2004;16:4160–7.
- [35] Rothstein SN, Federspiel WJ, Little SR. A simple model framework for the prediction of controlled release from bulk eroding polymer matrices. *J Mater Chem* 2008;18:1873–80.
- [36] Borden M, Attawia M, Khan Y, Laurencin CT. Tissue engineered microsphere-based matrices for bone repair: design and evaluation. *Biomaterials* 2002;23:551–9.
- [37] Meyer U, Wiesmann HP. Bone and cartilage engineering. Berlin Heidelberg: Springer; 2006.
- [38] Hong Z, Zhang P, Liu A, Chen L, Chen X, Jing X. Composites of poly(lactide-co-glycolide) and the surface modified carbonated hydroxyapatite nanoparticles. *J Biomed Mater Res A* 2007;81:515–22.